Journal of Translational Autoimmunity 10 (2025) 100284

Contents lists available at ScienceDirect

Journal of Translational Autoimmunity

journal homepage: www.sciencedirect.com/journal/journal-of-translational-autoimmunity

Leucine enhances the cGAS-STING-NLRP3 pathway in autoimmune thyroiditis

Xin Shen [a,e,1], Tingting Feng [b,1], Shangbin Li [f], Xingxin Wang [e], Wenhui Zhang [e], Shouyan Wang [c], Xiaohan Zhang [b], Jiguo Yang [e,*], Yuanxiang Liu [d,**]

[a] Department of General Practice, Shandong Provincial Hospital Affiliated to Shandong First Medical University, Jinan, Shandong Province, 250021, China
[b] Shandong Provincial Hospital Affiliated to Shandong First Medical University, Jinan, Shandong Province, 250021, China
[c] Heze Municipal Hospital, Heze, Shandong Province, 274000, China
[d] The First Clinical Medical College, Shandong University of Traditional Chinese Medicine, Jinan, Shandong Province, 250355, China
[e] School of Acupuncture-Moxibustion and Tuina, Shandong University of Traditional Chinese Medicine, Jinan, Shandong Province, 250355, China
[f] Department of Health Office, Shandong Provincial Hospital Affiliated to Shandong First Medical University, Jinan, Shandong Province, 250021, China

ARTICLE INFO

Handling editor: Y Renaudineau

Keywords:
Autoimmune thyroiditis
cGAS
Leucine
Mendelian randomisation
NLRP3
STING

ABSTRACT

Background: Branched-chain amino acids (BCAAs), including isoleucine (Ile), leucine (Leu), and valine (Val), are substrates for synthesising nitrogenous compounds and signalling molecules involved in regulating immunity. To date, data on the role of BCAAs in autoimmune thyroiditis (AIT) are lacking; therefore, this study aimed to determine the causality using two-sample Mendelian randomisation (MR) and explored the role of BCAAs in the cGAS-STING-NLRP3 pathway *in vitro*.

Methods: The causal relationship between BCAAs and the pathogenesis of AIT were identified using a two-sample MR study. The anti-inflammatory effects of BCAAs and their role in the cGAS-STING-NLRP3 pathway were investigated in lipopolysaccharide (LPS)- induced thyroid follicular cells (TFCs).

Results: Our findings indicate that BCAAs are a pathogenic factor for AIT (IVW OR = 4.960; 95 % CI = (1.54,15.940); $P = 0.007$). Leu significantly exacerbated the inflammatory response of thyroid cells, as evidenced by the up-regulation of tumour necrosis factor-alpha (TNF-α) and interleukin (IL)-6 and down-regulation of TGF-β1; simultaneously aggravated cellular injury and oxidative stress; significantly increased the expression of Sestrin2/p-mTOR and cGAS/STING/NLRP3 in AIT cells. Furthermore, the expression of IL-18 and IL-1β was significantly increased. Conversely, Leu deprivation induced cell injury, decreased oxidative stress, and inhibited Sestrin2/p-mTOR and cGAS/STING/NLRP3 pathways.

Conclusion: Our findings suggest a potential causal effect of genetically predicted Leu on AIT; Leu significantly exacerbated the inflammatory response and cellular damage in AIT cells. The mechanism by which Leu induces inflammation involves activating the promoted Sestrin2/mTOR and cGAS-STING-NLRP3 signalling pathways. Our study proposes a novel mechanism for the contributions of Leu in AIT and potential therapeutic strategies involving Leu deprivation in treating AIT.

List of Abbreviations

Abbreviation	Full Term
AIT	Autoimmune thyroiditis
BCAAs	Branched chain amino acids
cGAMP	cyclic GMP-AMP
cGAS	cyclic GMP-AMP synthase
Ile	isoleucine
Leu	leucine
Leu-de	Leu deprivation

(*continued on next column*)

(*continued*)

(*continued on next page*)

* Corresponding author.
** Corresponding author.
E-mail addresses: sdyangjiguo@126.com (J. Yang), lyxlwtg@126.com (Y. Liu).
[1] These authors contributed equally to this work.

https://doi.org/10.1016/j.jtauto.2025.100284
Received 14 January 2025; Received in revised form 12 March 2025; Accepted 15 March 2025
Available online 22 March 2025

(*continued*)

Abbreviation	Full Term
LDH	Lactate dehydrogenase
LPS	lipopolysaccharide
MDA	Malondialdehyde
mTOR	mammalian target of rapamycin
ROS	Reactive Oxygen Species
SOD	Superoxide Dismutase
STING	Stimulator of interferon genes
TFCs	thyroid follicular cells
Val	valine

1. Introduction

Autoimmune thyroiditis (AIT), an organ-specific autoimmune disease with 20–30 % of patients developing hypothyroidism, is the leading cause of hypothyroidism in iodine-sufficient areas worldwide [1]. Lymphocyte infiltration (especially T lymphocytes) into the thyroid gland and destruction of thyroid follicles are the primary pathological features of AIT, leading to various systemic symptoms, such as constipation, rough skin, atherosclerosis, bradycardia, anaemia, increased female abortion rate, Hashimoto's encephalopathy, and increased risk of thyroid cancer [2–5]. The immune imbalance and attack by thyroid autoimmune antibodies induced by genetic and environmental factors are the primary contributors to AIT. To date, specific treatment remains lacking [6].

Epidemiological studies have demonstrated the close link between nutritional factors, especially protein intake [7]and the occurrence and development of AIT; however, the mechanism of action of amino acids in AIT remains nebulous. Branched-chain amino acids (BCAAs) are a class of amino acids found in α Amino acids containing branched side chains on carbon, including isoleucine (Ile), leucine (Leu), and valine (Val). BCAAs are the substrates for the synthesis of nitrogenous compounds; they also serve as signalling molecules regulating the metabolism of glucose, lipid, and protein synthesis, intestinal health, and immunity via a special signalling network, especially phosphoinositide 3-kinase-protein kinase B (PI3K-AKT), mammalian target of rapamycin (mTOR) [8]. BCAAs play important roles in the physiological regulation of insulin resistance, type 2 diabetes, cardiovascular diseases, diabetes mellitus, and immunity and are involved in immune function regulations, including increasing fuel sources for immune cells and $CD4^+$, $CD4^+/CD8^+$, intestinal immunoglobulins, innate and adaptive immune responses, proinflammatory cytokines, and dendritic cell function [9–12]. However, there are no studies on the involvement of BCAAs in the mechanism of AIT. This study aimed to determine whether BCAAs are involved in the pathogenesis of AIT, whether intervening with branched-chain amino acids can treat AIT, and the specific mechanisms involved.

AIT is an organ-specific autoimmune disease in which abnormal alterations in the thyroid are a major contributor to the immune system's loss of tolerance. The initiation of a thyroid-associated natural immune response may be an upstream link in the imbalance of lymphocyte differentiation [13].

Cyclic GMP-AMP synthase (cGAS), a double-stranded DNA (dsDNA) recognition receptor expressed primarily in the cytosol, recognises dsDNA of pathogenic origin and dsDNA fragments of its abnormal cellular origin. Upon cGAS recognition of abnormal dsDNA in the cytosol, it dimerises and catalyses the formation of cyclic GMP-AMP (cGAMP) from intracellular adenosine triphosphate and guanosine triphosphate. cGAMP is a secondary messenger that binds to the stimulator of interferon genes (STING). STING is an endoplasmic reticulum transmembrane junction protein expressed in various tissue types and a key component of the natural immune response against cytoplasmic dsDNA [14]. Accumulating evidence indicates that the cGAS-STING signalling pathway plays a vital role in innate immunity and is a key regulator of adaptive immunity, hence connecting innate and adaptive immunity [15]. cGAS-STING can also modulate the cell death programme, the NLRP3 inflammasome in acute kidney injury [16], Alzheimer's disease [17], and myelodysplastic syndromes [18].

Studies investigating AIT have shown that NLRP3 activation can secrete cytokines such as interleukin (IL)-18 and IL-1β, thereby triggering inflammatory cascades, regulating lymphocytes, and leading to an imbalance in lymphocyte differentiation. This exacerbates the damage to thyrocytes; therefore, blocking the cGAS-STING-NLRP3 pathway may be a promising treatment for AIT.

To determine whether BCAAs were involved in the pathogenesis of AIT, we first explored the causal relationship between BCAAs and AIT using a two-sample Mendelian randomisation (MR) study. Subsequently, to elucidate the mechanism underlying the involvement of BCAAs in the pathogenesis of AIT via the cGAS-STING-NLRP3 pathway and whether BCAA deficiency has a therapeutic effect on AIT, we conducted experiments on thyroid cells. To the best of our knowledge, this study is the first to explore the relationship between amino acids and the pathogenesis of AIT. The findings of this study will facilitate the development of novel therapeutic strategies for AIT.

2. Materials and methods

2.1. Two-sample MR analysis between BCAAs and AIT

2.1.1. Study design and data sources

Our bidirectional, two-sample MR study conducted in this study is illustrated in Fig. 1.

Statistics used for the association of genetic variation with exposure and the association of genetic variation with outcomes were extracted from two separate non-overlapping published GWAS.

Sources for BCAAs and AIT Leu sample data were obtained from the IEU open GWAS (https://gwas.mrcieu.ac.uk/datasets/met-c-897/), a database with a sample size of 24,925 and a total of 12, 133, 295 SNP loci was obtained from IEU open GWAS (https://gwas.mrcieu.ac.uk/datasets/ebi-a-GCST90092995/), a database with a sample size of 115,082and a total of 11, 590, 399 SNP loci. Ile sample data were obtained from IEU open GWAS (https://gwas.mrcieu.ac.uk/datasets/ebi-a-GCST90092843/), a database with a sample size of 115,079and a total of 11, 590, 399 SNP loci. AIT sample data were obtained from IEU open GWAS (https://gwas.mrcieu.ac.uk/datasets/ebi-a-GCST90018635/), a database with a sample size of 173,193 (observer group: 537; control group: 172,656) and a total of 12, 453, 732SNP loci.

2.1.2. Genetic instrument selection

We filtered exposed instrumental variables based on the following conditions: (1) To prove the first MR assumption, we filtered SNPs associated with exposure at a level of genome-wide significance ($P < 5 \times 10^{-8}$); (2) to exclude the effect of linkage disequilibrium between SNPs and ensure the SNPs are independent, we set linkage disequilibrium (LD) clumping by setting $r^2 < 0.001$ or clump distance >1,0000 kb; (3) to testify the second hypothesis, we used the PhenoScanner to identify SNPs with significant association strengths. The PhenoScanner database was used to exclude genetic instrumental variables associated with confounders, focusing on excluding phenotypes associated with the outcomes. As previously reported [19], the confounding factors identified were iodine intake, selenium and Vitamin D levels, and stress. Single SNPs with phenotypic or outcome correlations were excluded from the analysis.

2.1.3. Two sample MR

We performed a two-way MR analysis of the BCAAs and AIT. MR analysis uses genetic variations as instrumental variables (IV) to estimate the causal association between exposure and outcomes. We used five commonly used data regression methods, including MR-Egger, weighted median, inverse variance weighted (IVW), simple mode, and

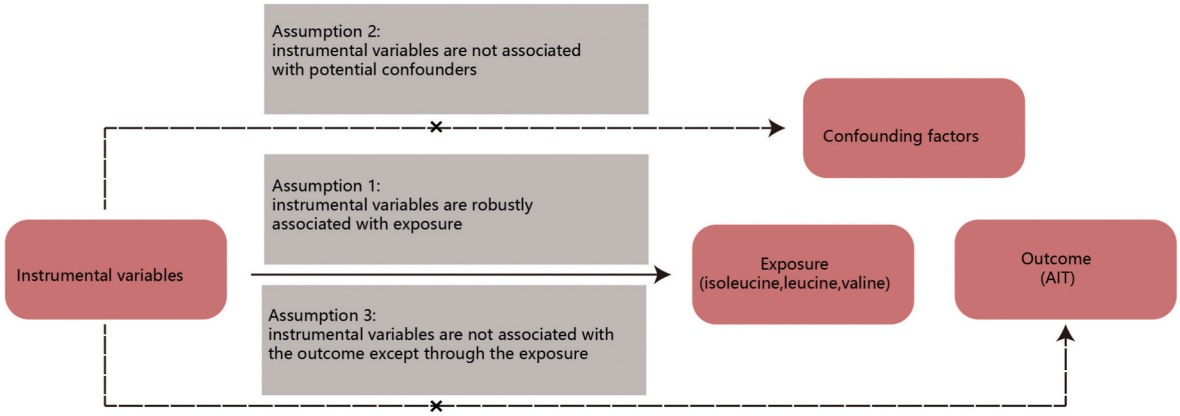

Fig. 1. Assumptions of two-sample Mendelian randomisation analysis between BCAAs and AIT.

weighted mode, which are also installed in the "TwoSampleMR version 0.5.7" package.

Heterogeneity among SNPs was assessed using Cochran's Q and funnel tests, and leave-one-out analysis was used to determine whether there was a single SNP that could affect the results of the causal assessment. These statistical analyses were performed using the open-source software R (version 4.3.1) and the R package "TwoSampleMR" (version 0.5.7). TwoSampleMR" (version 0.5.7). Differences were considered statistically significant at $P < 0.05$.

2.2. Experimental study of leu to alleviate inflammation in AIT

2.2.1. Reagents

The following reagents were used: DMEM1640 (Gibco, catalogue number: C11875500BT), foetal bovine serum (Gibco, catalogue number: A5256701), TNF-α (QuantiCyto, catalogue number: EHC103a), IL-6 (QuantiCyto, catalogue number: EHC007), IL-1β (QuantiCyto, catalogue number: EHC002b), IL-18 (Elabscience, catalogue number: E-EL-H0253) Cellular Malondialdehyde (MDA) Assay Kit (Nanjing Jianjian Bioengineering Research Institute, catalogue number: A003-1-2), Total Superoxide Dismutase (SOD) Assay Kit (Nanjing Jianjian Bioengineering Research Institute, catalogue number: A001-1-2), Lactate dehydrogenase (LDH) cytotoxicity assay kit (Biyun Tian Biologicals Inc.; catalogue number: C0016), Reactive Oxygen Species (ROS) Assay Kit (Biyun Tian Biologicals Inc.: S0033S), cGAS (HUABIO, catalogue number: HA500023), STING (Protein Tech, catalogue number: 19851-1-AP), NLRP3 (cat 27458-1-AP, Proteintech, China), Caspase-1 (db3022, Diagbio, China), GSDMD (db7773, Diagbio, China).

2.2.2. Cell culture and treatments

The Nthy-ori 3–1 cell line was obtained from the China Centre Type Culture Collection. Cells were cultured in normal RPMI 1640 medium and 10 % foetal bovine serum in a humidified atmosphere containing 5 % CO_2. Cells between passages five and eight were used in all experiments. The cells were then divided into the following four groups:

1. Normal control (Con) group: cells were cultured in a normal medium for 24 h, and the cell culture supernatant was replaced by a normal medium for 6 h.
2. AIT group: cells were cultured in a normal medium for 24 h, and the cell culture supernatant was replaced by a normal medium and treated with 10 μg/mL LPS and 100 mg/L NaI for 6 h.
3. AIT + Leu group: Cells were cultured in a normal medium for 24 h, and cell culture supernatant was replaced by a normal medium. The cells were treated with 10 μg/mL LPS, 100 mg/L NaI, and 5 nM Leu for 6 h.
4. AIT Leu deprivation (Leu-de) group: Cells were cultured in a normal medium for 24 h, and cell culture supernatant was replaced by Leu-free medium. The cells were treated with 10 μg/mL LPS (Sigma) and 100 mg/L NaI for 6 h.

2.2.3. Determination of TNF-α, IL-6, IL-1β, and IL-18

The standard was diluted according to the required concentration; 30x of the concentrated biotinylated antibody was diluted into a 1x working solution, prepared 20 min before use, and stored in the dark at room temperature. To the required slats, the standard and specimen common diluent were added to the blank wells. The sample and various concentrations of the standard were added to the remaining wells. To each well, 100 μL was added, and the reaction wells were sealed with adhesive sealing paper and placed in a 37 °C incubator for 90 min in the dark. The plate was washed five times, then the biotinylated antibody diluent was added to the blank wells and the biotinylated antibody working solution was added to the remaining wells. Again, 100 μL was added to each well, new sealing paper was used to seal the plate, and the biotinylated antibody working solution was added to each well. The reaction wells were sealed with new sealing tape and incubated at 37 °C for 60 min in the dark. The plate was washed five times and the enzyme conjugate dilution solution was added to the blank wells while the enzyme conjugate working solution to the remaining wells. To each well, 100 μL was added, the reaction wells were sealed with new sealing tape and incubated at 37 °C for 30 min in the dark. The plate was washed again five times before adding the colour substrate and incubating for 15 min, then adding the colour substrate and incubating for 15 min. After incubation for 15 min, 100 μL of termination solution was added to each well and mixed. The absorbance of the cells was measured at 450 nm with an enzyme meter immediately. A standard curve was plotted, and the concentration of each group of samples was calculated.

2.2.4. Determination of intracellular ROS levels

DCFH-DA was diluted with serum-free culture medium at 1:1000 to produce a final concentration of 10 μmol/L. Cells were collected, suspended in diluted DCFH-DA at a concentration of one to 20 million cells/mL, and incubated for 20 min at 37 °C in an incubator. Mixing was performed via an upside–down motion every 3–5 min to ensure full contact between the probe and the cells. The cells were washed three times with serum-free cell culture medium to adequately remove DCFH-DA that had not entered the cells and observed using fluorescence microscopy.

2.2.5. Measurement of LDH, MDA, and SOD activities

Measurement of LDH activity: An appropriate number of cells was inoculated into a 96-well plate according to the cell size and growth rate so that the cell density did not exceed 80–90 % when the cells were to be detected. According to the manufacturer's instructions, 60 μL of prepared LDH assay working solution was added to each well, mixed well by blowing, and incubated for 30 min at room temperature in the dark.

The absorbance was measured at 490 nm, and the absorbance of each measured group was subtracted from the absorbance of the background blank control wells. Cytotoxicity or mortality (%) = (Absorbance of treated samples – Absorbance of sample control wells)/(Absorbance of maximal enzyme activity of cells – Absorbance of sample control wells) × 100.

Measurement of MDA activity: An appropriate number of cells was inoculated into a 96-well plate and grouped into drug treatments; the supernatant was discarded, the cells were scraped with a cell scraper, transferred into the EP tube, reagent V extract was added (0.5 mL), and mixed well by blowing. An ultrasonic crusher was used to break the cells into a suspension, of which 0.1 mL was added into a new EP tube; a small hole was created on the cap of the new EP tube and marked well. The cover lid was added, mixed using a vortex mixer, and placed in a 95 °C water bath for 40 min. The EP tube was placed under running water to cool, and then centrifugated at 4000 rpm for 10 min, and scanned at 530 nm using ELISA plate reader to configure the reaction solution.

Calculation formula: MDA content (nmoL/mgprot) = (measured OD value – blank OD value)/(standard OD value - blank OD value) × standard concentration (10 nmoL/mL) ÷ sample protein concentration (mgprot/mL).

Measurement of SOD was performed by inoculating the appropriate amount of cells into a 6-well plate, adding trypsin (0.5 mL) to each well, and digesting for 2 min at room temperature. A complete medium (1 mL) was added to terminate the digestion and mixed well by blowing. The liquid was aspirated and transferred to a new EP tube and centrifuged at 1000 rpm for 10 min; the supernatant was discarded, and 1 mL of LPS was added to the bottom of the precipitated cells, mixed well by blowing, and centrifuged at 1000 rpm for 10 min; the supernatant was discarded.

PBS (1 mL) was added, mixed well, and centrifuged at 1000 rpm for 10 min; the supernatant was discarded. The protein concentration was determined using the bicinchoninic acid (BCA) method. The SOD working solution was prepared according to the instruction manual, and according to the grouping, it was added to the 96-well plate, mixed well, and incubated at 37 °C for 20 min. The absorbance was measured at 490 nm using an enzyme marker.

Calculation formula: SOD inhibition (%) = (A control - A control blank) - (A assay - A assay blank)/(A control – A control blank) × 100 %; SOD activity (U/mgprot) = SOD inhibition ÷ 50 % × reaction system (0.24 mL)/dilution (0.02 mL) ÷ protein concentration of the sample to be tested (mgprot/mL).

2.2.6. Western blot analysis

The protein levels of cGAS, STING, NLRP3, GSDMD, caspase-1, and Sestrin2 in thyroid follicular cells (TFCs) were detected using western blotting. Protein concentration was determined using a BCA protein quantification kit. Proteins were separated at a constant voltage of 110 V in the 10 % geland transferred onto a PVDF membrane. After blocking with 5 % skimmed milk, the membrane was incubated overnight at 4 °C with the primary antibody diluted in the blocking solution. PVDF membranes were washed with TBST before antibody incubation and after and after blocking with milk. On the following day, the membrane was incubated with horseradish peroxidase-conjugated secondary antibody for an additional 1 h. Densitometric values indicate relative target protein expression levels normalised to values for β-actin/GAPDH on the same membrane. Immunoreactive proteins were reacted with enhanced chemiluminescence solution after washing, and colour was developed using the SuperSignal West Pico chemiluminescent substrate.

2.2.7. Statistical analysis

Statistical analyses were performed using SPSS 22.0 software. Quantitative variables are presented as the means ± standard deviations (SD). Student's *t*-test was used to analyze the differences between two groups. Comparisons among groups were conducted using one-way ANOVA. If the data did not meet the normality assumption, the Wilcoxon rank-sum test was used. Differences were considered statistically significant at $P < 0.05$.

3. Results

3.1. Instrumental variable determination

In this study, SNP loci of genetic variables associated with Leu, Val, and Ile with genome-wide significance ($P < 5 \times 10^{-8}$) were selected for pooling, and SNPs that simultaneously satisfied hypotheses 1, 2, and 3 were screened to obtain 3, 15, and 8 hypothesis-conformant SNPs, respectively. SNPs with significant associations with the outcome AIT were removed using the PhenoScanner database (n = 0), and the data for the outcome AIT were extracted by GWAS to obtain significant associations of the above SNPs with the outcome. The exposure and outcome datasets were merged, and SNPs with chain imbalance and palindromic structure were removed. The results of the MR analysis are shown in Table 1.

3.2. Causal effect of BCAAs on AIT from MR analysis

The results of the MR analysis suggested that Leu increases the risk of AIT. As shown in Table 1 and Fig. 2A, the IVW method provided primary causal evidence of Leu involvement in AIT (OR = 4.960, 95 % CI: 1.54–15.940, SE = 0.596, $P < 0.05$). However, As shown in Table 1 and Fig. 2B and C, the causal association between circulating Val and Ile levels and the risk of AIT was not significant; the *P*-values of the IVW method were 0.102 and 0.455. Scatterplots of the MR analysis are shown in Fig. 2D–F.

Subsequently, a sensitivity analysis of the results of Leu in AIT was performed. Cochran's Q test was used to assess heterogeneity, and the *P*-values of the Q statistics calculated in the Cochran's Q test of IVW and MR-Egger were 0.373 and 0.179, respectively, indicating no significant heterogeneity of the included SNPs. We used the same method to perform a sensitivity analysis of the results of Val and Ile in AIT.

The *P*-values of the Q statistics calculated using the Cochran Q test for IVW and MR-Egger were 0.579 and 0.561 and 0.09 and 0.133.

For horizontal pleiotropy, the *P*-values of the MR-Egger intercept of Leu, Val, and Ile on AIT were 0.810, 0.404, and 0.266, respectively ($P > 0.05$), indicating no horizontal pleiotropy and that the instrumental variables did not influence the outcome through pathways other than exposure.

Table 1
The MR results of BCAAs on AIT.

Outcome	Exposure	Methods	N. SNPs	OR	SE	*P*
AIT	Leucine	MR Egger	3	46.878	7.363	0.693
		Weighted median	3	4.193	0.668	0.032
		Inverse variance weighted	3	4.960	0.596	0.007
		Simple mode	3	5.887	1.030	0.227
		Weighted mode	3	3.173	0.700	0.241
	Valine	MR Egger	15	3.433	0.799	0.147
		Weighted median	15	1.591	0.511	0.363
		Inverse variance weighted	15	1.877	0.385	0.102
		Simple mode	15	2.010	0.891	0.446
		Weighted mode	15	1.644	0.503	0.339
	Isoleucine	MR Egger	8	30.112	2.425	0.210
		Weighted median	8	2.216	0.777	0.305
		Inverse variance weighted	8	1.768	0.762	0.455
		Simple mode	8	4.276	1.647	0.407
		Weighted mode	8	2.601	0.903	0.325

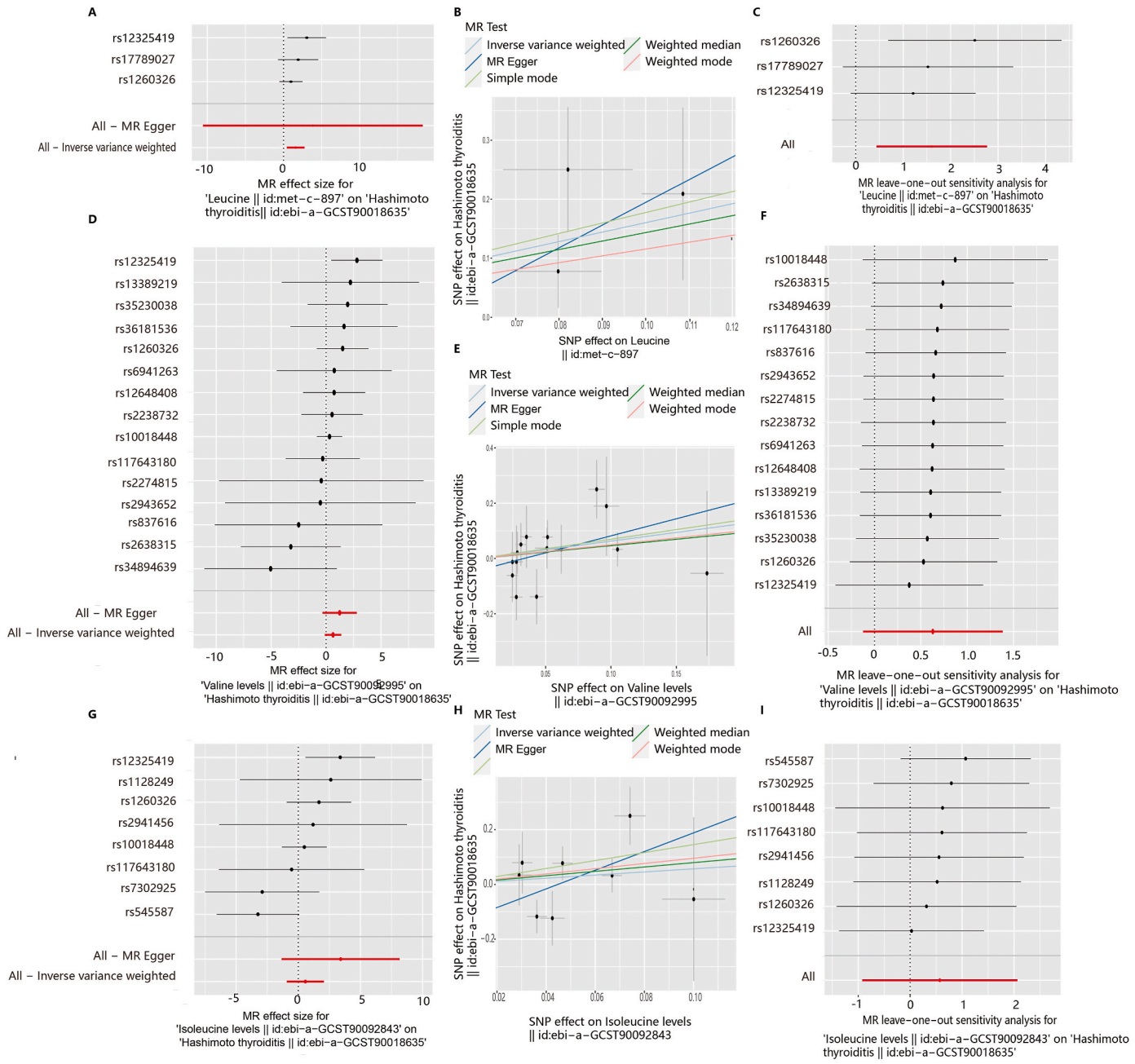

Fig. 2. Causal effect of BCAAs on AIT from MR analysis. A. MR effect for Leucine on AIT; B. MR effect for Valine on AIT; C. MR effect for Isoleucine on AIT; D. Scatter plot of the causal relationship of Leucine on AIT; E. Scatter plot of the causal relationship of Valine on AIT; F. Scatter plot of the causal relationship of Isoleucine on AIT; G. MR leave-one-out sensitivity analysis of Leucine on AIT; H.MR leave-one-out sensitivity analysis of Valine on AIT; I.MR leave-one-out sensitivity analysis of Isoleucine on AIT.

The leave-one-out of Leu, Val, and Ile on AIT showed no outliers that significantly affected the results of the MR analysis (Fig. 2G–I).

3.3. Leu accelerates apoptosis of thyroiditis cells

To explore the role of Leu in thyroid cell damage, we examined the level of apoptosis in the cells subjected to different treatments. As shown in Fig. 3A and B, compared with the Con group (4.22 ± 0.37), IFN-γ stimulation increased the apoptosis level of thyroid cells (10.83 ± 0.61, $P < 0.05$) by 2.57 times higher than the Con group. Compared with the AIT group, the addition of Leu increased the apoptosis percentage (20.78 ± 4.22, $P < 0.05$) by 1.92 times. Leu deprivation treatment alleviated the apoptosis percentage (5.78 ± 2.21, $P < 0.05$), which was 53 % of that observed in the AIT group.

3.4. Leu exacerbates inflammatory response of thyroiditis cells

To verify the effect of Leu on thyroid cell inflammation, we examined the levels of cellular inflammatory factors in each group. As shown in Fig. 3C and D, IFN-γ stimulation significantly increased TNF-α (22.51 ± 5.81) and IL-6 (6.65 ± 0.36) compared with the Con group (TNF-α11.16 ± 0.52, IL-6 4.41 ± 0.13, $P < 0.05$ or $P < 0.01$). Additional Leu stimulation further increased TNF-α (44.35 ± 0.88) IL-6 (10.34 ± 0.18) compared with the AIT group (TNF-α22.51 ± 5.81, IL-6 6.65 ± 0.36, $P < 0.05$), whereas the lack of Leu group showed a significant decrease of TNF-α (14.18 ± 1.06, $P < 0.05$), and IL-6 (5.71 ± 0.37, $P < 0.05$). We

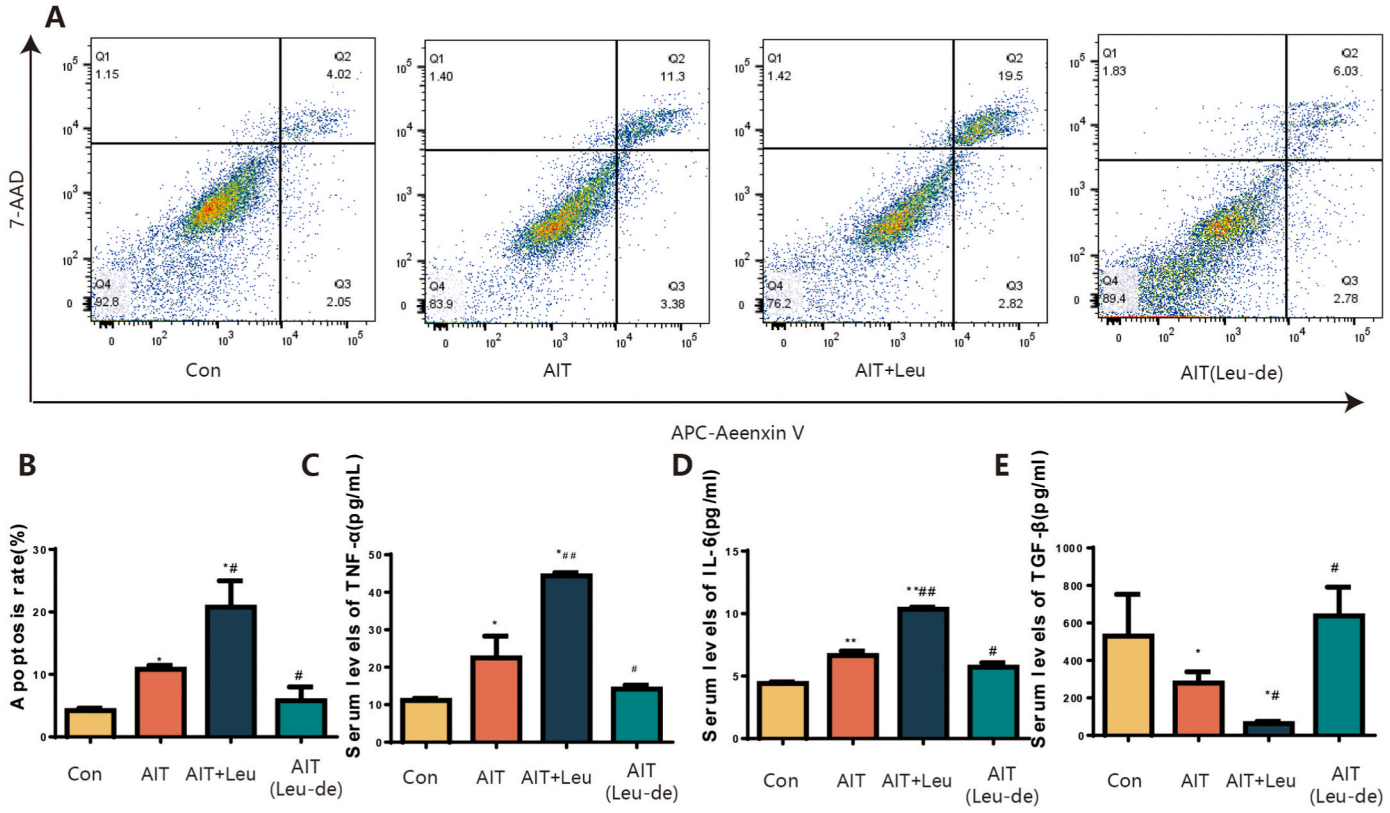

Fig. 3. Leucine exacerbates apoptosis and inflammatory factor secretion. A. Flow cytometry detection of apoptotic cells; B. Statistical analysis of apoptotic cells; C. Levels of TNF-α in different groups detected by ELISA assay; D. Levels of IL-6 in different groups detected by ELISA assay; E. Levels of TGF-β1 in different groups detected by ELISA assay. n = 3, compared with Con,$^{*}P < 0.05$; compared with AIT, $^{\#}P < 0.05$, $^{\#\#}P < 0.01$.

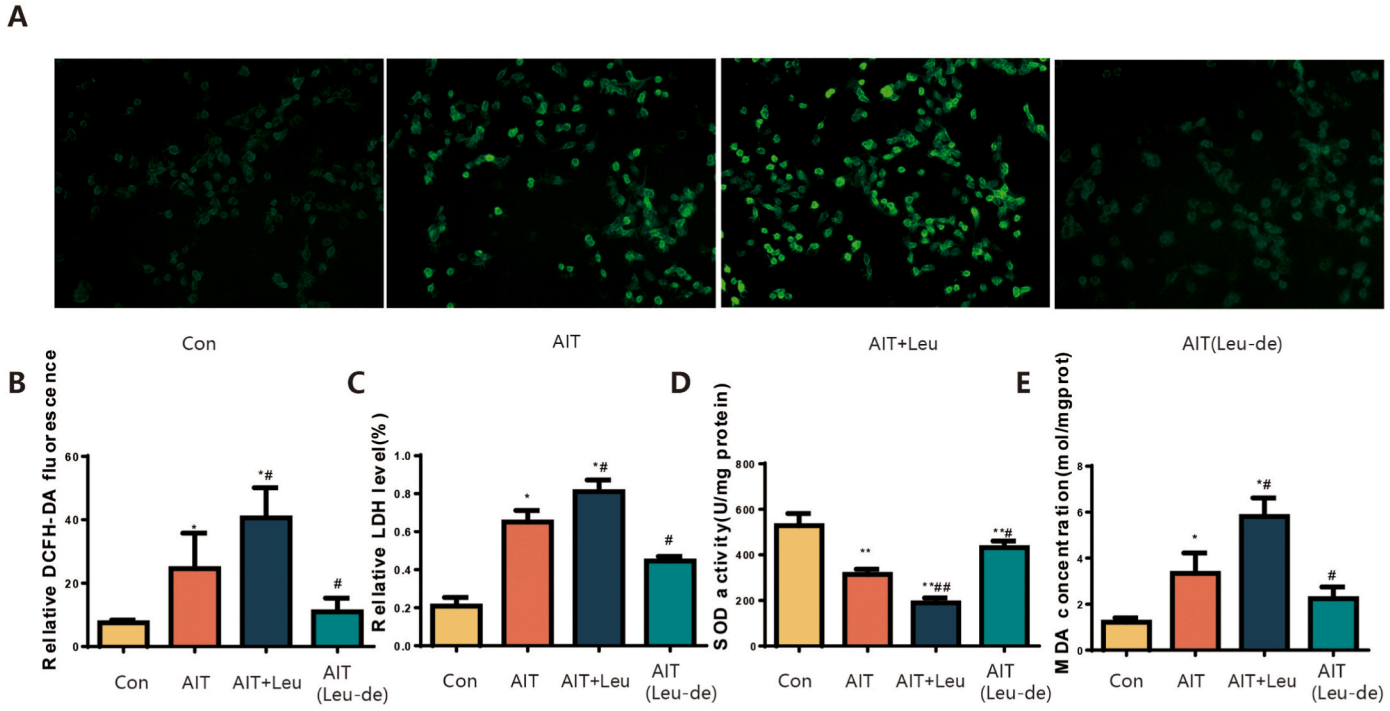

Fig. 4. Leucine promotes oxidative stress in AIT cells. A.Detection of ROS in thyroid cells by immunofluorescence assay. B. Quantitative statistical analysis of ROS probes (DCFH-DA) in AIT cells. C. The LDH release in AIT cells. The content of SOD(D) and MDA(E) in AIT cells. n = 3, compared with Con,$^{*}P < 0.05$; compared with AIT, $^{\#}P < 0.05$, $^{\#\#}P < 0.01$.

also examined TGF-β1 levels (Fig. 3E), a cytokine that suppresses immune function, and showed it was decreased in the AIT group (278.61 ± 60.32, $P < 0.05$) and continued to decrease with the addition of Leu (63.09 ± 11.52, $P < 0.05$); the lack of Leu group showed a significant increase in TGF-β1 (637.93 ± 153.50, $P < 0.05$).

3.5. Leu aggravates oxidative stress response of thyroiditis cells

Oxidative stress indirectly reflects cell damage. The present study examined the expression levels of ROS in the thyroid cells of each group. As shown in Fig. 4A–E, IFN-γ injury significantly reduced SOD (313.66 ± 23.01) compared with the Con group (528.58 ± 53.21, $P < 0.01$) and accumulated ROS (28.04 ± 10.80), LDH (0.65 ± 0.06), and MDA (3.34 ± 0.89) compared the Con group (ROS 7.61 ± 1.01, LDH 0.21 ± 0.05, MDA 1.22 ± 0.19, $P < 0.05$), which were adverse phenomena of oxidative stress and indirectly reflected cell damage. Additional Leu stimulation further decreased SOD (189.58 ± 21.89, $P < 0.05$) and increased ROS (42.32 ± 10.85, $P < 0.05$), LDH (0.81 ± 0.06, $P < 0.05$) and MDA (5.81 ± 0.82, $P < 0.05$) compared with the AIT group. However, compared with the AIT group, Leu deprivation reversed the changes in the above indicators (SOD 431.62 ± 29.67, ROS 9.13 ± 2.96, LDH0.45 ± 0.02, MDA2.25 ± 0.51, $P < 0.05$).

3.6. Leu enhances Sestrin2 and p-mTOR expression

Sestrin2 is an important receptor for sensing Leu levels. Leu binding to Sestrin2 is vital in activating intracellular mTORC1, modulating various biological processes, such as mitochondrial biogenesis, nucleotide synthesis, mRNA translation (protein synthesis), lipid synthesis, and autophagy. As shown in Fig. 5A and B, Leu-induction of Sestrin2 (1.01 ± 0.10) and p-mTOR (1.46 ± 0.08) increased compared with the AIT group (Sestrin2 0.68 ± 0.03, p-mTOR 1.14 ± 0.09, $P < 0.05$).

Conversely, Leu deprivation significantly decreased the expression of Sestrin2 (0.76 ± 0.05, $P < 0.05$) and p-mTOR (0.90 ± 0.05, $P < 0.05$).

3.7. Leu induces cGAS-STING-NLRP3 pathway activation in thyroiditis cells

As shown in Fig. 6A and B, IFN-γ stimulation significantly increased cGAS (0.82 ± 0.09) and STING (0.92 ± 0.10) compared with the Con group (cGAS 0.39 ± 0.03, STING 0.72 ± 0.06, $P < 0.05$). Additional Leu stimulation further increased cGAS (1.08 ± 0.03) and STING (1.24 ± 0.13) compared with the AIT group ($P < 0.05$), whereas Leu deprivation significantly decreased cGAS (0.77 ± 0.06, $P < 0.05$) and STING (0.93 ± 0.07, $P < 0.05$). As shown in Fig. 6C–E, additional Leu up-regulated the expression of NLRP3 (1.33 ± 0.17), GSDMD (1.30 ± 0.34), caspase-1 (1.54 ± 0.22), while Leu deprivation down-regulated NLRP3 (0.80 ± 0.07), GSDMD (0.68 ± 0.06), and caspase-1 (0.56 ± 0.05) compared with the AIT group (NLRP3 1.04 ± 0.09, GSDMD 0.81 ± 0.07, caspase-1 1.08 ± 0.16, $P < 0.05$). NLRP3 activation secretes IL-18 and IL-1β, further triggering inflammatory cascade responses that regulate lymphocytes and lead to an imbalance in lymphocyte differentiation and further cellular attack. Therefore, these two inflammatory factors were also detected. As shown in Fig. 6F, additional Leu enhanced the expression of IL-18 (42.33 ± 0.74, $P < 0.05$) and IL-1β (91.73 ± 18.68, $P < 0.05$), while Leu deprivation diminished these two cytokines (IL-18 5.36 ± 0.44, IL-1β 23.12 ± 2.16, $P < 0.05$) compared with the AIT group (IL-18 18.25 ± 0.93, IL-1β 55.73 ± 12.67).

4. Discussion

In this study, we explored the therapeutic effects of BCAAs on AIT and showed that Leu increased the risk of AIT, exacerbated inflammation in AIT thyroid cells, aggravated cellular damage, and promoted cGAS-STING-NLRP3 pathway levels. However, Leu deprivation reversed these effects, suggesting targeting Lue immunometabolic pathways as a treatment strategy for AIT (Fig. 7).

In this study, we first explored BCAA levels and the risk of developing AIT using MR analysis. We excluded SNPs with genetic pleiotropy by the PhenoScanner database and MR-Egger regression modelling and found no heterogeneity. Following Bonferroni correction, the IVW model results indicated a significant causal association between elevated Leu levels and an increased risk of AIT. In addition, the results of the leave-one-out sensitivity analysis outlined the robust assessment of the causal association between the two.

In contrast, we observed no causal association between the Ile and Val levels and AIT risk. Notably, the significant causal association between Leu levels and AIT risk was validated owing to the limited number of SNPs. We also determined whether Leu could promote AIT inflammation and elucidated the possible mechanisms.

AIT is an imbalance in immune homeostasis caused by a combination of genetic and environmental factors with pathological features that include serum autoantibodies against thyroid antigens, lymphocytic infiltration of the thyroid gland, apoptosis, necrosis, and eventual progression to thyroid failure [20]. The breakdown of immune tolerance and the attack of self-reactive $CD4^+$T lymphocytes on their thyroid tissue are important pathogenesis factors in AIT. Production of inflammatory factors IFN-γ, IL-1β, and TNF-α and chemokines by $CD4^+$T cells can recruit more inflammatory cells towards the thyroid tissues, which forms an inflammatory microenvironment of the thyroid gland and damages thyroid cells [20]. In this study, we constructed an *in vitro* cellular model of AIT based on previous methods [21]. The inflammatory cell cytokines, such as TNF-α and IL-6, of thyroid cells following LPS stimulation were significantly elevated, while TGF-β1, which can inhibit the expression of immune cells, was significantly decreased, consistent with previous findings [21], suggesting that the construction of an *in vitro* disease model of AIT was successful. The levels of these inflammatory factors were further increased by culturing AIT cells in media containing excess Leu, whereas Leu starvation decreased inflammatory factors in AIT cells. These results suggested that Leu exacerbates AIT inflammation, whereas Leu deprivation alleviates it.

Next, we evaluated the effects of Leu on cellular damage, including apoptosis and oxidative stress. Our results demonstrated that Leu exacerbated AIT cell injury, whereas Leu deprivation attenuated AIT

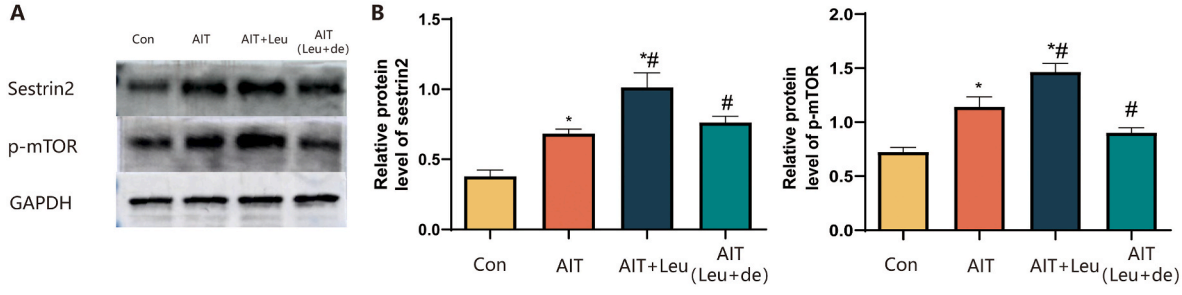

Fig. 5. Representative Western blotting analyze of Sestrin2 and p-mTOR (A and B). n = 3, compared with Con,*$P < 0.05$; compared with AIT, $^{\#}P < 0.05$.

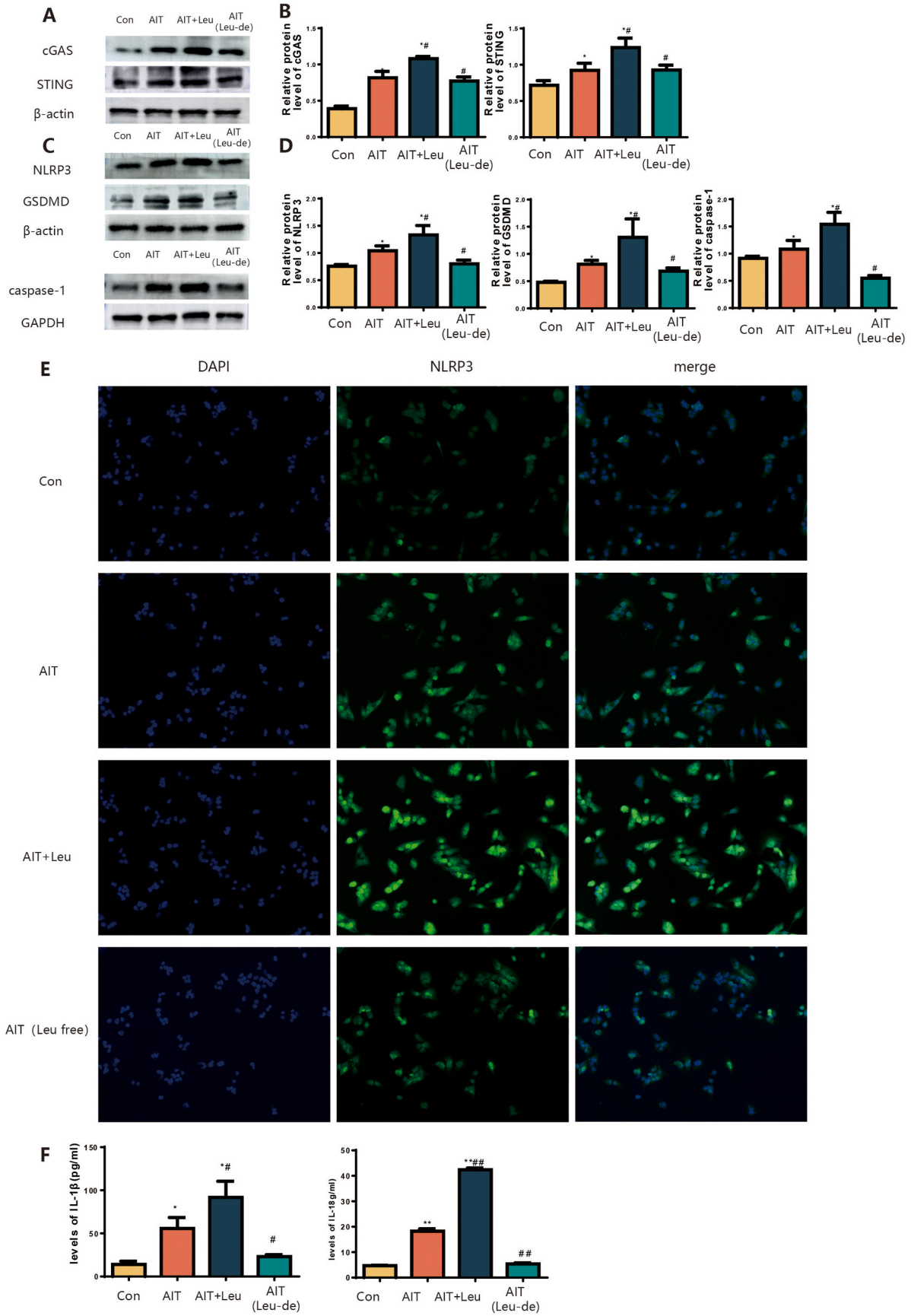

Fig. 6. Representative Western blotting analyze of cGAS and STING (A and B). Representative Western blotting analyze of NLRP3,GSDMD and caspase-1 (C and D).E. Immunofluorescence detection of NLRP3 expression level in AIT cells. F. Detection of IL-1β and IL-18 Expression Levels in AIT by ELISA. n = 3, compared with Con,* $P < 0.05$, *$P < 0.01$; compared with AIT, $^{\#}P < 0.05$, $^{\#}P < 0.01$.

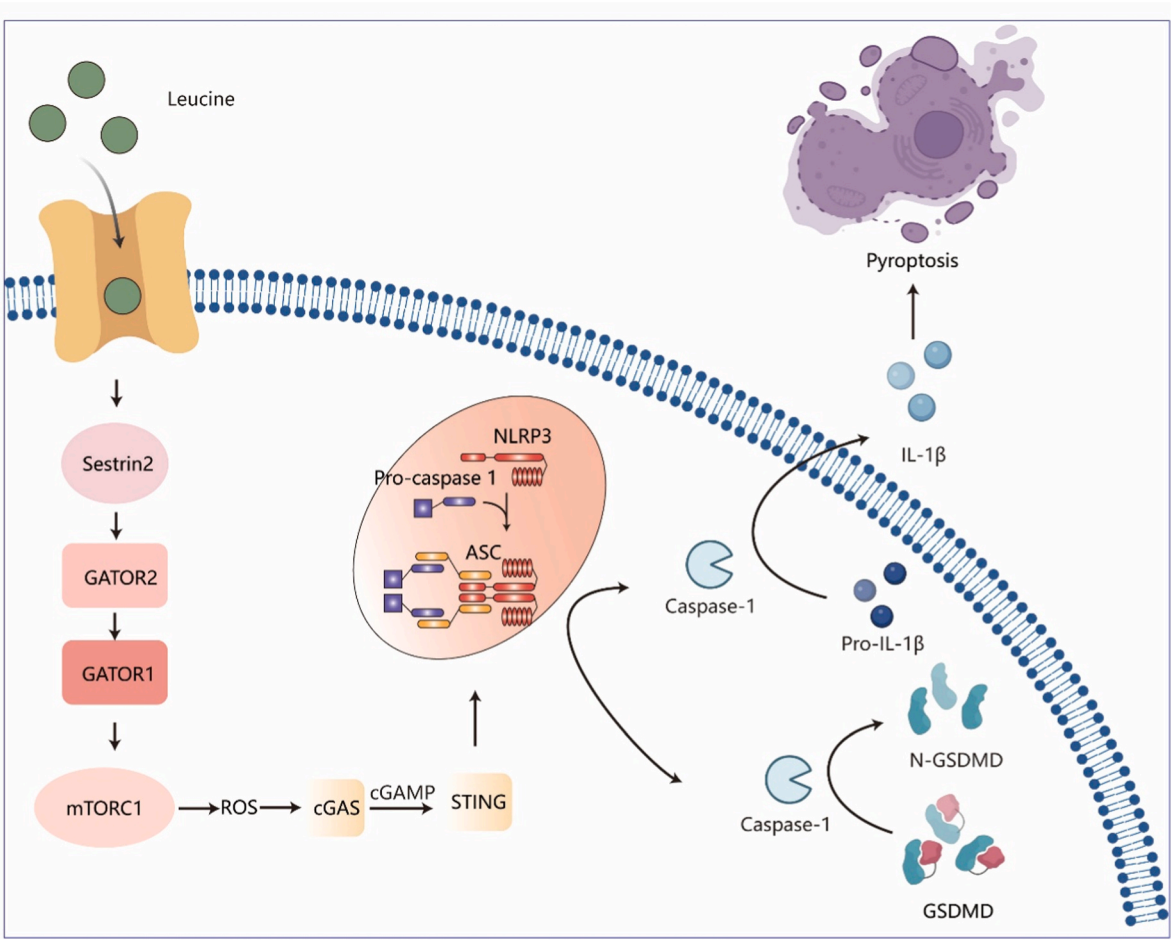

Fig. 7. Leucine accelerate cGAS-STING-NLRP3 pathway in autoimmune thyroiditis

apoptosis. Furthermore, Leu increased ROS levels in AIT cells, suggesting that Leu induced cellular oxidative stress, as illustrated by Leu-induced increases in LDH and MDA levels and a decrease in SOD levels. We further explored the mechanisms leading to an increase in ROS levels. Recent studies have shown that in most cell types, including neurones, Leu inhibits autophagy by activating mTORC1 [22]. A decrease in autophagy leads to a reduction in ROS clearance, ultimately resulting ROS accumulation and inducing cell damage [23]. Sestrin2 is an important receptor for sensing Leu levels [24]; when Leu binds to Sestrin2, it is released from the complex of the mTORC1 regulator GATOR2, activating the mTORC1 complex [25].

We speculate that Leu induces oxidative stress by inhibiting autophagy via the Sestrin2/mTOR pathway activation, leading to ROS accumulation. Our results suggest that Leu can induce oxidative stress via Sestrin2/mTOR, leading to cellular damage and that Leu deprivation reverses these effects.

Kawashima et al. have suggested AIT as a classic organ-specific autoimmune disease, that abnormal alterations in the thyroid are major contributors to the immune system's loss tolerance to it, and that the initiation of thyroid-associated natural immune responses are an upstream link in the imbalance of lymphocyte differentiation [13].

As a novel and vital innate immune signalling pathway, the cGAS-STING signalling pathway, activated by nucleic acid substances, interacts with other immune responses and participates in regulating cancer, autoimmune and inflammatory diseases, and microbial and parasitic infectious diseases, among other diseases [15]. The release of mitochondrial DNA (mtDNA) mediated by ROS is an important signal for activating the cGAS-STING pathway [26,27]. The cGAS-STING signalling pathway triggered by nucleic acids is involved in the pathogenesis of various autoimmune diseases, including systemic lupus erythematosus, osteoarthritis and rheumatoid arthritis [28,29].

cGAS-STING-dependent type I IFN responses drive T lymphocytes to mediate cellular inflammation and autoantibody responses, including $CD4^+$ and $CD8^+$ T cells. cGAS is involved in AIT; hence, it is a promising target. Our results showed that Leu induced the expression of cGAS and STING, whereas Leu deprivation decreased the expression of these proteins. This indicates that Leu promotes cGAS/STING and cGAS activations, possibly by promoting ROS accumulation and activating the cGAS/STING pathway.

cGAS-STING can regulate the cell death programme [30]. The reciprocal regulation of inflammasome and cGAS-STING signalling pathway has been well documented [31]. cGAMP catalysed by cGAS directly activates NLRP3, causing it to oligomerise and assemble with ASC and pro caspase-1 to form inflammasomes. The expression of NLRP3 inflammasome is increased in thyroid tissues of AIT patients, and the inflammasome initiates inflammatory response and expands the inflammatory cascade in the autoimmune pathogenesis of AIT through the activation of post-translational modifications of cytokines, such as IL-18 and IL-1β mediated by caspase-1, and the death of thyroid cells by pyroptosis [32].

These two pathways regulate lymphocytes and inhibit lymphocyte differentiation, further triggering inflammatory cascade responses [32]. In the present study, Leu promoted NLRP3 inflammasome activation and elevated IL-18 and IL-1β, as well as the expression of GSDMD and caspase-1, suggesting that Leu promotes NLRP3 inflammasome-mediated Pyroptosis and its deficiency reverses these changes. This confirms that Leu exacerbates thyroiditis cell inflammation and cell damage, and that cGAS-STING-NLRP3 signalling is an

essential pathway for Leu to exert its pro-inflammatory effect on the inflammatory response.

This study has some limitations. Although our results demonstrated the effects of Leu on the inflammatory response associated with the cGAS-STING-NLRP3 signalling pathway, further validation remains warranted using cGAS/STING-knockout or NLRP3-knockout mice. Other regulatory enzymes that may play crucial roles in the metabolic pathways of Leu remain to be investigated.

The present study confirmed that Leu increased risk of contracting AIT. The findings indicated that Leu significantly exacerbated the inflammatory response and cellular damage in AIT cells. The mechanism by which Leu induces inflammation is associated with the activation of the Sestrin2/mTOR and cGAS-STING-NLRP3 signalling pathways. This study proposes a novel mechanism for the pathogenesis and treatment of AIT as well as Leu deprivation as a therapeutic strategy against AIT. The findings presented in this study will facilitate future nutrition-related studies on protein intake in patients with AIT.

CRediT authorship contribution statement

Xin Shen: Writing – original draft, Validation, Methodology, Formal analysis. **Tingting Feng:** Writing – review & editing, Resources, Methodology. **Shangbin Li:** Methodology, Formal analysis. **Xingxin Wang:** Software, Investigation. **Wenhui Zhang:** Software, Investigation. **Shouyan Wang:** Methodology, Formal analysis. **Xiaohan Zhang:** Software, Investigation. **Jiguo Yang:** Writing – review & editing, Supervision, Resources, Project administration, Funding acquisition, Conceptualization. **Yuanxiang Liu:** Writing – review & editing, Supervision, Resources, Project administration, Funding acquisition, Conceptualization.

Funding sources

This study was supported by the National Natural Science Foundation of China. [grant number: 82405099].

Declaration of competing interest

The authors declare that they have no known competing financial interests or personal relationships that could have appeared to influence the work reported in this paper.

Acknowledgements

We thank all the technicians at the Experimental Animal Centre of Shandong Provincial Hospital for their assistance.

Data availability

Data will be made available on request.

References

[1] F. Ragusa, P. Fallahi, G. Elia, D. Gonnella, Hashimotos' thyroiditis: e pidemiology, pathogenesis, clinic and therapy, Best Pract. Res. Clin. Endocrinol. Metabol. 33 (6) (2019) 101367, https://doi.org/10.1016/j.beem.2019.101367.

[2] A.P. Weetman, An update on the pathogenesis of Hashimoto's thyroiditis, J. Endocrinol. Investig. 44 (5) (2020) 883–890, https://doi.org/10.1007/s40618-020-01477-1.

[3] U. Feldt-Rasmussen, Hashimoto's thyroiditis as a risk factor for thyroid cancer, Curr. Opin. Endocrinol. Diabetes Obes. 27 (5) (2020) 364–371, https://doi.org/10.1097/med.0000000000000570.

[4] M. Ralli, D. Angeletti, M. Fiore, Hashimoto's thyroiditis: an update on pathogenic mechanisms, diagnostic protocols, therapeutic strategies, and potential malignant transformation, Autoimmun. Rev. 19 (10) (2020) 102649, https://doi.org/10.1016/j.autrev.2020.102649.

[5] E.K. Konte, H. Karakas, N. Akay, Evaluation of thyroid dysfunction in childhood-onset systemic lupus erythematosus: risk factors for Hashimoto's thyroiditis, Lupus 33 (11) (2024) 1235–1241, https://doi.org/10.1177/09612033241272964.

[6] Q.B. Martinez, C. Yazbeck, L.B. Sweeney, Thyroiditis: evaluation and treatment, Am. Fam. Physician 104 (6) (2021) 609–617.

[7] P. Ihnatowicz, M. Drywień, P. Wątor, The importance of nutritional factors and dietary management of Hashimoto's thyroiditis, Ann. Agric. Environ. Med. 27 (2) (2020) 184–193, https://doi.org/10.26444/aaem/112331.

[8] C. Nie, T. He, W. Zhang, Branched chain amino acids: beyond nutrition metabolism, Int. J. Mol. Sci. 19 (4) (2018) 954, https://doi.org/10.3390/ijms19040954.

[9] J.-P. De Bandt, X. Coumoul, R. Barouki, Branched-Chain amino acids and insulin resistance, from protein supply to diet-induced obesity, Nutrients 15 (1) (2022) 68, https://doi.org/10.3390/nu15010068.

[10] P.J. White, R.W. McGarrah, M.A. Herman, J.R. Bain, Insulin action, type 2 diabetes, and branched-chain amino acids: a two-way street, Mol. Metabol. 52 (2021) 101261, https://doi.org/10.1016/j.molmet.2021.101261.

[11] Z. Li, Y. Wang, H. Sun, The role of branched-chain amino acids and their metabolism in cardiovascular diseases, J. Cardiovasc. Transl. Res. 17 (1) (2024) 85–90, https://doi.org/10.1007/s12265-024-10479-w.

[12] B. Yahsi, G. Gunaydin, Immunometabolism – the role of branched-chain amino acids, Front. Immunol. 13 (2022), https://doi.org/10.3389/fimmu.2022.886822.

[13] A. Kawashima, K. Tanigawa, T. Akama, Innate immune activation and thyroid autoimmunity, J. Clin. Endocrinol. Metabol. 96 (12) (2011) 3661–3671, https://doi.org/10.1210/jc.2011-1568.

[14] A. Decout, J.D. Katz, S. Venkatraman, The cGAS–STING pathway as a therapeutic target in inflammatory diseases, Nat. Rev. Immunol. 21 (9) (2021) 548–569, https://doi.org/10.1038/s41577-021-00524-z.

[15] L. Ou, A. Zhang, Y. Cheng, The cGAS-STING pathway: a promising immunotherapy target, Front. Immunol. 12 (2021), https://doi.org/10.3389/fimmu.2021.795048.

[16] X. Luo, Y. Zhao, Y. Luo, Cytosolic mtDNA–cGAS–STING axis contributes to sepsis-induced acute kidney injury via activating the NLRP3 inflammasome, Clin. Exp. Nephrol. 28 (5) (2024) 375–390, https://doi.org/10.1007/s10157-023-02448-5.

[17] D. Gao, J. Hao, B. Li, Tetrahydroxy stilbene glycoside ameliorates neuroinflammation for Alzheimer's disease via cGAS-STING, Eur. J. Pharmacol. 953 (2023) 175809, https://doi.org/10.1016/j.ejphar.2023.175809.

[18] A.F. McLemore, H.-A. Hou, B.S. Meyer, Somatic gene mutations expose cytoplasmic DNA to co-opt the cGAS/STING/NLRP3 axis in myelodysplastic syndromes, JCI Insight 7 (15) (2022), https://doi.org/10.1172/jci.insight.159430.

[19] W. Cyna, A. Wojciechowska, W. Szybiak-Skora, The impact of environmental factors on the development of autoimmune thyroiditis—review, Biomedicines 12 (8) (2024) 1788. https://doi.org/10.3390/biomedicines12081788.

[20] K. Wrońska, M. Hałasa, M. Szczuko, The role of the immune system in the course of hashimoto's thyroiditis: the current state of knowledge, Int. J. Mol. Sci. 25 (13) (2024) 6883, https://doi.org/10.3390/ijms25136883.

[21] Q. Guo, H. Qu, H. Zhang, Prunella vulgaris L. Attenuates experimental autoimmune thyroiditis by inhibiting HMGB1/TLR9 signaling, Drug Des. Dev. Ther. 15 (2021) 4559–4574, https://doi.org/10.2147/dddt.s325814.

[22] S.M. Son, S.J. Park, E. Stamatakou, Leucine regulates autophagy via acetylation of the mTORC1 component raptor, Nat. Commun. 11 (1) (2020), https://doi.org/10.1038/s41467-020-16886-2.

[23] Y. Xie, G. Zhao, X. Lei, Advances in the regulatory mechanisms of mTOR in necroptosis, Front. Immunol. 14 (2023), https://doi.org/10.3389/fimmu.2023.1297408.

[24] V. Panwar, A. Singh, M. Bhatt, Multifaceted role of mTOR (mammalian target of rapamycin) signaling pathway in human health and disease, Signal Transduct. Targeted Ther. 8 (1) (2023), https://doi.org/10.1038/s41392-023-01608-z.

[25] R.L. Wolfson, L. Chantranupong, R.A. Saxton, Sestrin2 is a leucine sensor for the mTORC1 pathway, Science 351 (6268) (2016) 43–48, https://doi.org/10.1126/science.aab2674.

[26] X.M. Ma, K. Geng, B.Y.-K. Law, Lipotoxicity-induced mtDNA release promotes diabetic cardiomyopathy by activating the cGAS-STING pathway in obesity-related diabetes, Cell Biol. Toxicol. 39 (1) (2022) 277–299, https://doi.org/10.1007/s10565-021-09692-z.

[27] Z. Liu, M. Wang, X. Wang, XBP1 deficiency promotes hepatocyte pyroptosis by impairing mitophagy to activate mtDNA-cGAS-STING signaling in macrophages during acute liver injury, Redox Biol. 52 (2022) 102305, https://doi.org/10.1016/j.redox.2022.102305.

[28] Q. Feng, X. Xu, S. Zhang, cGAS-STING pathway in systemic lupus erythematosus: biological implications and therapeutic opportunities, Immunol. Res. 72 (6) (2024) 1207–1216, https://doi.org/10.1007/s12026-024-09525-1.

[29] X. Yang, L. Zhao, Y. Pang, cGAS-STING pathway in pathogenesis and treatment of osteoarthritis and rheumatoid arthritis, Front. Immunol. 15 (2024), https://doi.org/10.3389/fimmu.2024.1384372.

[30] J. Liu, X. Zhang, H. Wang, The cGAS-STING-mediated NLRP3 inflammasome is involved in the neurotoxicity induced by manganese exposure, Biomed. Pharmacother. 154 (2022) 113680, https://doi.org/10.1016/j.biopha.2022.113680.

[31] N.-S.-Y. Yang, W.-J. Zhong, H.-X. Sha, mtDNA-cGAS-STING axis-dependent NLRP3 inflammasome activation contributes to postoperative cognitive dysfunction induced by sevoflurane in mice, Int. J. Biol. Sci. 20 (5) (2024) 1927–1946, https://doi.org/10.7150/ijbs.91543.

[32] Q. Guo, Y. Wu, Y. Hou, Cytokine secretion and pyroptosis of thyroid follicular cells mediated by enhanced NLRP3, NLRP1, NLRC4, and AIM2 inflammasomes are associated with autoimmune thyroiditis, Front. Immunol. 9 (2018), https://doi.org/10.3389/fimmu.2018.01197.